ELSEVIER

Journal of Applied Geophysics 46 (2001) 217–233

JOURNAL OF APPLIED GEOPHYSICS

www.elsevier.nl/locate/jappgeo

Analysis and interpretation of anomalous conductivity and magnetic permeability effects in time domain electromagnetic data
Part I: Numerical modeling

Dmitriy A. Pavlov, Michael S. Zhdanov *

Department of Geology and Geophysics, College of Mines and Earth Sciences, University of Utah, Room 719, 135 S 1460 E, Salt Lake City, UT 84112-0111, USA

Received 11 January 2000; accepted 8 March 2001

Abstract

Time domain electromagnetic (TDEM) response is usually associated with eddy currents in conductive bodies, since this is the dominant effect. However, other effects, such as displacement currents from dielectric processes and magnetic fields associated with rock magnetization, can contribute to TDEM response. In this paper we analyze the effect of magnetization on TDEM data. We use a 3-D code based on finite-difference method, developed by Wang and Hohmann [Geophysics 58 (1993) 797], to study transient electromagnetic field propagation through a medium containing bodies with both anomalous conductivity and anomalous magnetic permeability. The remarkable result is that the combination of anomalous conductivity and permeability within the same body could increase significantly the anomalous TDEM response in comparison with purely conductive or purely magnetic anomalies. This effect has to be taken into account in interpretation of TDEM data over electrical inhomogeneous structures with potentially anomalous magnetic permeability.

Keywords: Conductivity; Permeability; Modeling; Time-domain electromagnetic method

1. Introduction

Time domain electromagnetic (TDEM) method is one of the most widely used techniques in electromagnetic geophysical exploration. It is based on studying the response of the transient electromagnetic field in a geological cross-section. This response is usually associated with eddy currents in conductive bodies, since this is the dominant effect. However, other effects, such as displacement currents from dielectric processes and magnetic fields associated with rock magnetization, can contribute to TDEM response. Note that dielectric effect may be of importance only at high frequencies, or at a very early time. This effect is usually neglected for the frequency and time ranges considered in traditional electromagnetic exploration methods.

The effect of magnetization can be significant over a wide range of frequencies and time. The effect in frequency domain has been studied in sev-

* Corresponding author. Fax: +1-801-581-7065.
E-mail address: mzhdanov@mines.utah.edu (M.S. Zhdanov).

0926-9851/01/$ - see front matter
PII: S0926-9851(01)00040-4

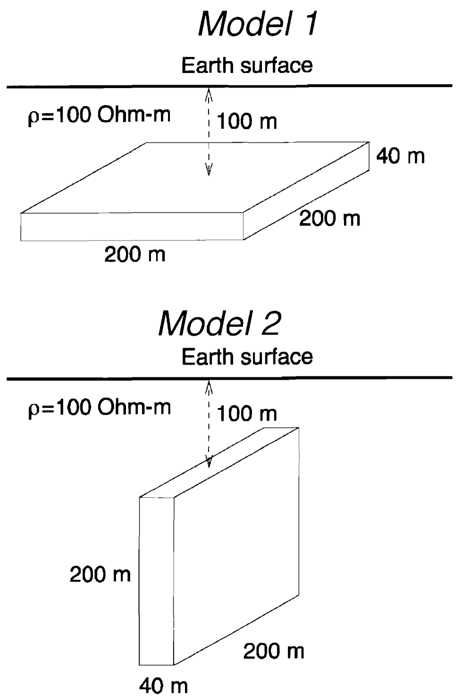

Fig. 1. Geoelectrical models for numerical modeling.

eral publications (Ward, 1959; Olhoeft and Strangway, 1974; Ward and Hohmann, 1988). Fraser (1981), discussed a method of using magnetic polarization response for mapping magnetite with a multicoil, multifrequency airborne electromagnetic system. Most of these results have been obtained based on a simple model of a conductive permeable sphere or conductive permeable cylinder in uniform space. In the recent paper by Zhang and Oldenburg (1999), more complex geoelectrical and geomagnetic models have been studied as well. The effect of magnetic permeability on the well logging measurements through metal casing has also been studied by several authors (see, for example, Strack et al., 1996; Kaufman et al., 1996).

The effect of magnetization on TDEM data as applied to mineral exploration problems, however, has not been discussed in the literature. At the same time this phenomenon could affect practical TDEM data.

In this paper, we use a powerful tool of numerical modeling based on finite-difference method (Wang and Hohmann, 1993), to study transient electromagnetic field propagation through a medium containing bodies with both anomalous conductivity and anomalous magnetic permeability.

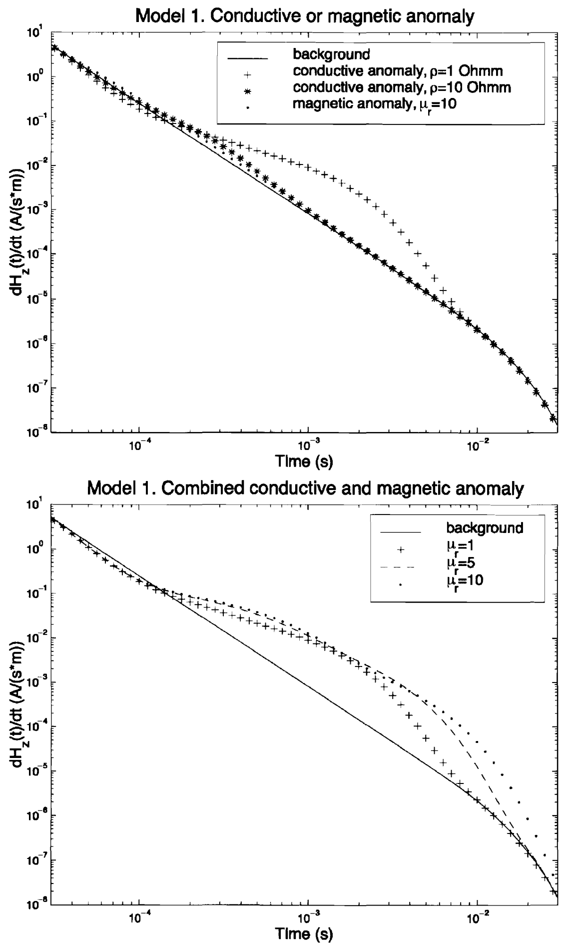

Fig. 2. Top panel: observed field $\partial H_z(t)/\partial t$ versus time above the center of the anomaly for Model 1 with purely conductive or magnetic anomaly. The solid line corresponds to the homogeneous half-space with a resistivity of 100 Ω m. The line formed by crosses shows the response for a purely conductive plate with a resistivity of 1 Ω m. The line formed by the stars is the magnetic response for a purely conductive plate with a resistivity of 10 Ω m. The dotted line represents the response for the case of a purely magnetic plate with $\mu_r = 10$. Bottom panel: observed field $\partial H_z(t)/\partial t$ versus time above the center of the anomaly for Model 1 with a combined conductive and magnetic anomaly with different magnetic permeabilities. The solid line corresponds to a homogeneous half-space with a resistivity of 100 Ω m. The line formed by crosses shows the response for a purely conductive plate with a resistivity of 1 Ω m. The dashed line represents the response from the combined anomaly with a resistivity of 1 Ω m and with a permeability of $\mu_r = 5$. The dotted line corresponds to the response from the combined anomaly with a resistivity of 1 Ω m and with a permeability of $\mu_r = 10$.

The remarkable result is that the combination of anomalous conductivity and permeability within the same body could increase significantly the anomalous TDEM response, in comparison with purely conductive or purely magnetic anomalies. This effect has to be taken into account in interpretation of the TDEM data over electrical inhomogeneous structures with potentially anomalous magnetic permeability. In a complimentary paper (Zhdanov and Pavlov, 2001), we develop a method of joint inversion of TDEM data with respect to conductive and magnetic anomalies.

2. Physical background

Incident electromagnetic fields generate several processes in geological target: eddy currents are induced in conductive bodies, and magnetic polarization is induced in magnetic bodies. According to Lenz's law, eddy currents tend to cancel the changes in the incident magnetic field B^{i}. The effect of the induced eddy current is strong enough in the early stage of the time domain electromagnetic process and becomes negligible in the later stages. The secondary magnetic field associated with magnetic

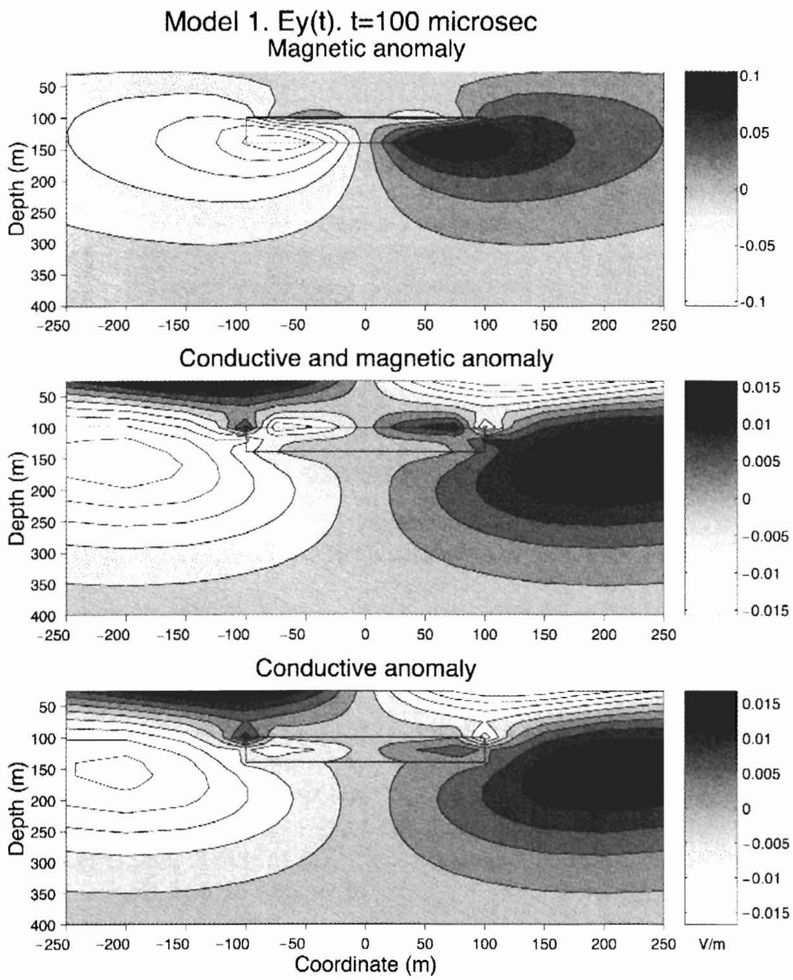

Fig. 3. Model 1. Snap-shots of the horizontal components of electrical field E_y (t, x, z) in the case of a horizontal plate for the time moment of 100 μs. The top panel corresponds to the case of a purely magnetic anomaly ($\rho_2 = \rho_1 = 100$ Ω m) with the relative magnetic permeability of the plate $\mu_r = 5$. The bottom panel presents the results for the case of a purely conductive anomaly ($\rho_2 = 1$ Ω m, $\mu_r = 1$), and the middle panel demonstrates the combined effect of magnetic and conductive anomalies ($\rho_2 = 1$ Ω m, $\mu_r = 5$).

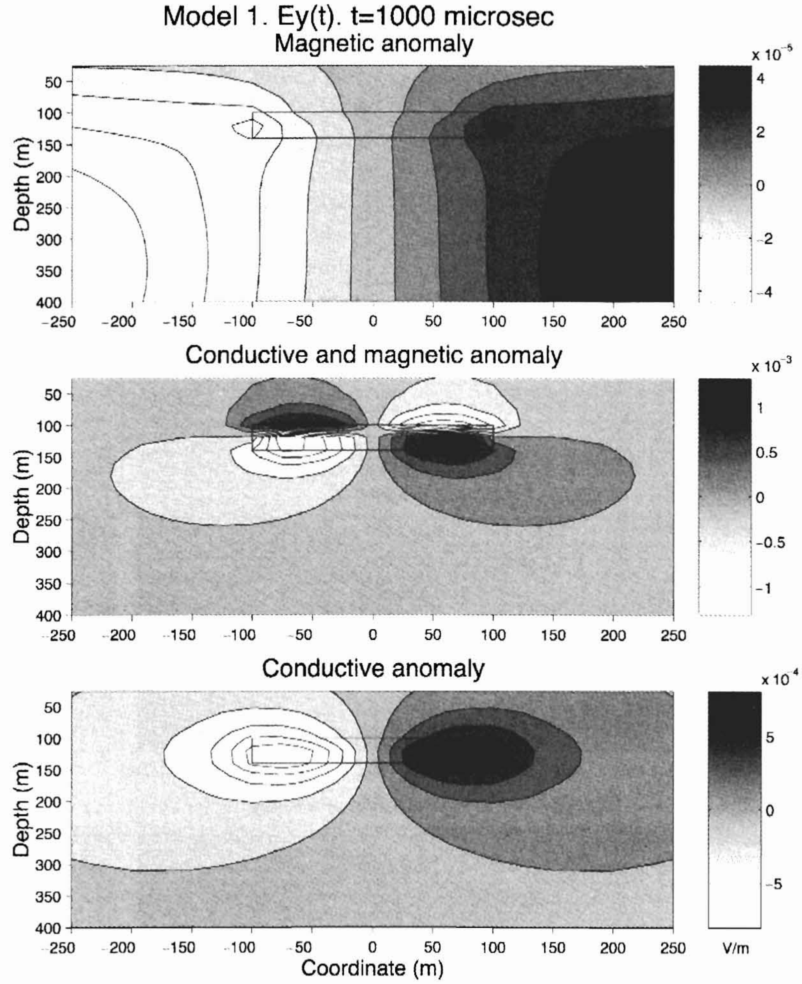

Fig. 4. Model 1. Plots of E_y (t, x, z) similar to Fig. 3 for the time moment of 1000 μs.

polarization phenomena can be significant over a much longer time period, because it is connected with the magnetic field itself, and not with its time derivative, as it follows from the physical properties of the magnetized body discussed below.

The magnetization vector $\boldsymbol{M}$ for linear and isotropic material is proportional to applied magnetic field H:

$$\boldsymbol{M} = \chi_m H, \tag{1}$$

where χ_m is the magnetic susceptibility. Note that the magnetic susceptibility of purely diamagnetic materials is negative, and in paramagnetic materials χ_m is positive. In diamagnetic materials the induced magnetic field tends to reduce the applied field, while in paramagnetic materials the induced field tends to increase the applied field. The susceptibility of ferromagnetic substances can be as large as 10^6, and therefore the applied field can increase dramatically.

The magnetic field B is equal to the superposition of vectors $\boldsymbol{M}$ and $\boldsymbol{H}$:

$$B = \mu_0(\boldsymbol{H} + \boldsymbol{M}) = \mu_0(1 + \chi_m)\boldsymbol{H} = \mu_0 \mu_r \boldsymbol{H} = \mu \boldsymbol{H}, \tag{2}$$

where

$$\mu_r = 1 + \chi_m \tag{3}$$

is relative permeability and

$$\mu = \mu_0 \mu_r \tag{4}$$

is the magnetic permeability of the material.

Values of relative permeability, for example, for a massive magnetite body are approximately $\mu_r = 5$ in extreme cases, while that of pyrrhotite may be $\mu_r = 1.25$ (Ward, 1959). Therefore, the incident magnetic field is typically increased significantly in magnetite rock formations.

Note that for the relatively small field generated in the TDEM method, we can assume that relative permeability is independent of the field strength.

Ward and Hohmann (Ward, 1959; Ward and Hohmann, 1988) have studied the frequency response of a conductive magnetic sphere in a uniform and plane wave magnetic field. They demonstrated that the response depends both on the conductivity and on the relative magnetic permeability of the sphere. Electromagnetic induction effects due to eddy currents are strong within a certain frequency range and usually decrease at low frequency. The magnetization effect is significant over a lower range of frequencies. These results were used in some subsequent publications for studying magnetite ore deposits.

In this paper, we analyze the combined effect of anomalous conductivity and anomalous permeability on an electromagnetic field in time domain. One can conduct a simple qualitative analysis of the basic

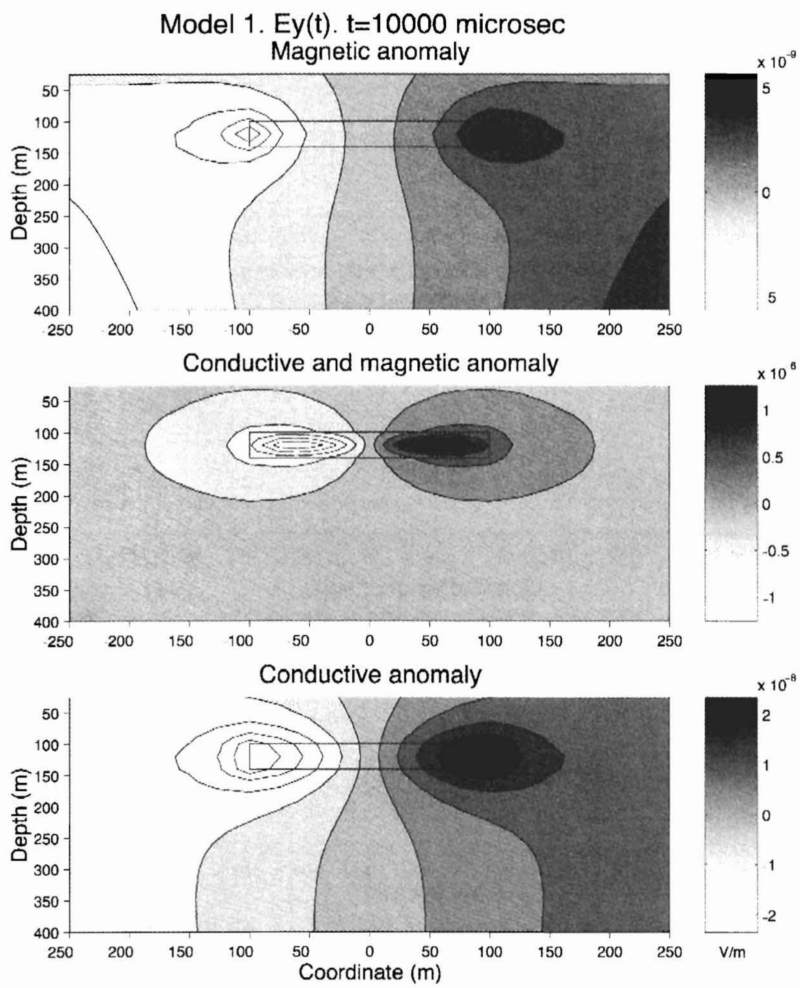

Fig. 5. Model 1. Plots of E_y (t, x, z) similar to Fig. 3 for the time moment of 10 000 μs.

equations of an electromagnetic field to examine this phenomenon. The underlying induction equation for an electric field, for example, is:

$$\mu \nabla \times \left(\frac{1}{\mu} \nabla \times E \right) + \mu \sigma \frac{\partial E}{\partial t} = -\mu \frac{\partial j^{e}}{\partial t}, \tag{5}$$

where j^{e} is the density of extraneous electric currents in the source. Taking into account formula (4), the last equation can be cast in the form

$$\nabla \times (\nabla \times E) - \nabla \ln \mu_{r} \times (\nabla \times E) + \mu_{0} \mu_{r} \sigma \frac{\partial E}{\partial t} = -\mu_{0} \mu_{r} \frac{\partial j^{e}}{\partial t}. \tag{6}$$

Eq. (6) contains two terms that can be affected by the anomalous permeability. The first term contains the gradient of the relative permeability, $\nabla \ln \mu_{r}$, and the second term includes the product of the relative

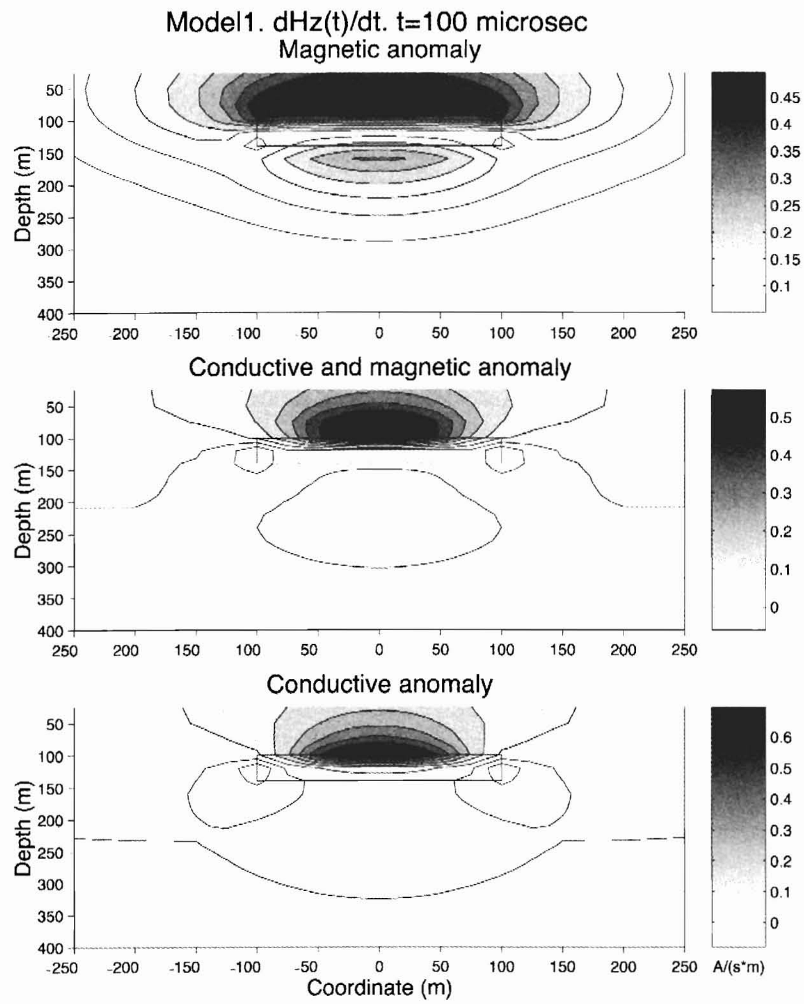

Fig. 6. Model 1. Snap-shots of the vertical components of magnetic field $H_z(t, x, z)/\partial t$ in the case of a horizontal plate for the time moment of 100 μs. The top panel corresponds to the case of a purely magnetic anomaly ($\rho_2 = \rho_1 = 100$ Ω m) with the relative magnetic permeability of the plate $\mu_r = 5$. The bottom panel presents the results for the case of a purely conductive anomaly ($\rho_2 = 1$ Ω m, $\mu_r = 1$), and the middle panel demonstrates the combined effect of magnetic and conductive anomalies ($\rho_2 = 1$ Ω m, $\mu_r = 5$).

permeability and conductivity, $\mu_r \sigma$. The first term reflects the effect of magnetic charges caused by magnetic inhomogeneities. In the case of the piecewise constant distribution of μ_r, these charges are concentrated on the boundaries of the anomalous body. The second term reflects the combined effects of both relative permeability and conductivity. The increased permeability or increased conductivity within same volume results in the same effect of increasing the volume density of eddy currents within an inhomogeneous domain. Therefore, we can distinguish between the anomalous permeability and anomalous conductivity effects only because of the boundary effect of the magnetic anomaly.

In order to conduct the quantitative comparative analysis of the anomalous conductivity and anomalous permeability effects on TDEM response, we apply numerical modeling technique.

3. Numerical modeling of time domain responses for 3-D bodies with anomalous conductivity and permeability

We consider the two typical models presented in Fig. 1. Model 1 (Fig. 1, top panel) consists of a horizontal rectangular plate with lateral dimensions

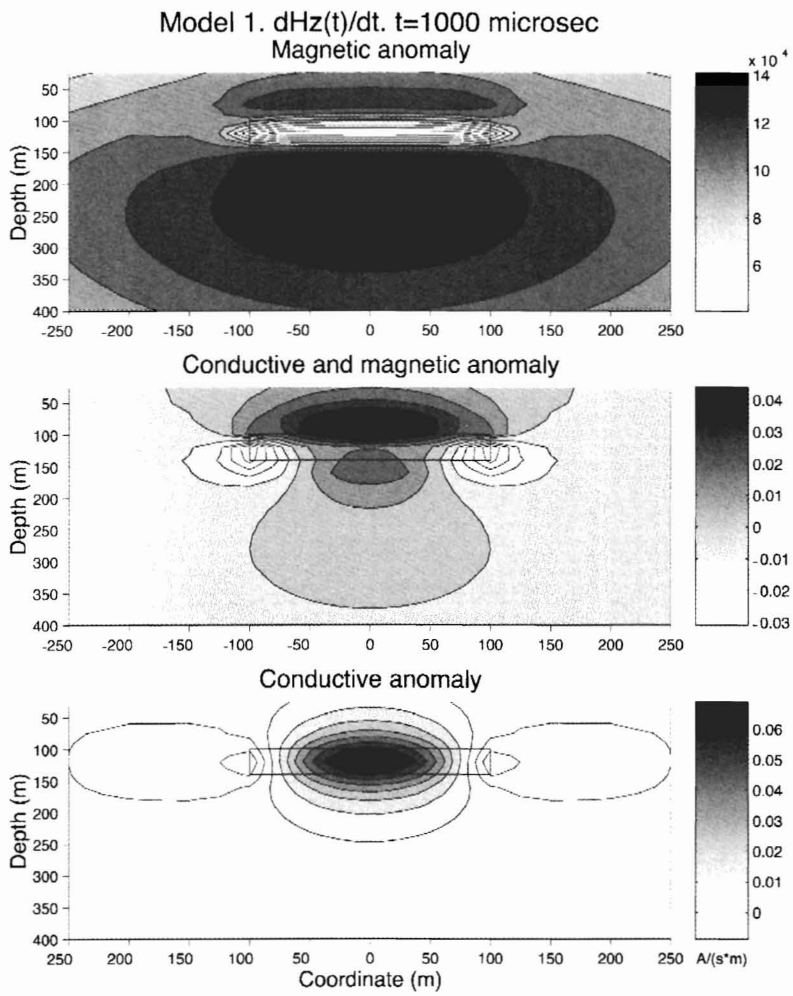

Fig. 7. Model 1. Plots of the vertical components of magnetic field $H_z(t, x, z)/\partial t$ similar to Fig. 6 for the time moment of 1000 μs.

200 × 200 m, and a thickness of 40 m, located at a depth of 100 m within a homogeneous, conductive half-space with a resistivity of $\rho_1 = 100\ \Omega$ m, and magnetic permeability of free space, μ_0. Model 2 (Fig. 1, bottom panel) consists of a vertical rectangular plate with lateral dimensions 40 × 200 m, and the vertical size 200 m, located at a depth of 100 m within the homogeneous, conductive half-space with resistivity of $\rho_1 = 100\ \Omega$ m, and magnetic permeability of free space, μ_0. We conducted a set of numerical experiments in which the relative permeability μ_r of the plate was equal subsequently to 1, 5 and 10, and the resistivity of the plate was set to be equal to the background resistivity $\rho_2 = 100\ \Omega$ m, or the plate was a good conductor: $\rho_2 = 1\ \Omega$ m, or $\rho_2 = 10\ \Omega$ m. The transient electromagnetic field in the model was generated by a step pulse of electric current in a rectangular loop of size 50 × 50 m, located on the ground above the center of the plate. Numerical modeling was conducted using time domain finite-difference code developed by Wang and Hohmann (1993).

The following three cases are studied:

1. the plate is characterized by anomalous magnetic permeability only (purely magnetic anomaly);
2. the plate is characterized by anomalous conductivity only (purely conductive anomaly); and

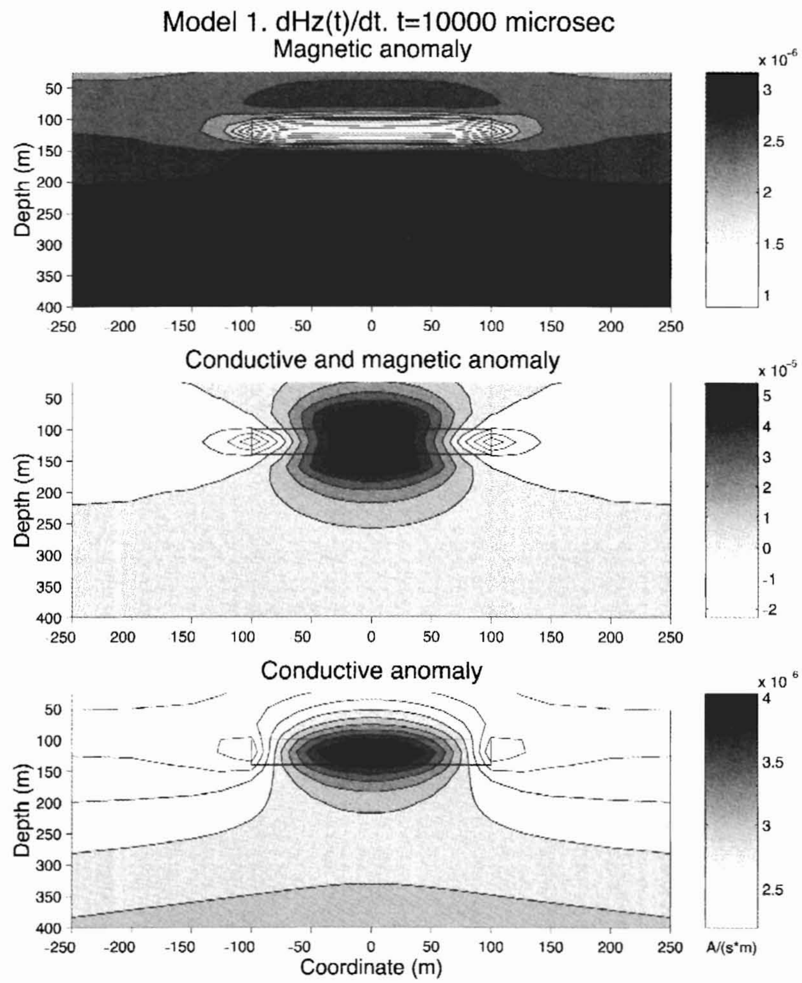

Fig. 8. Model 1. Plots of the vertical components of magnetic field $H_z(t, x, z)/\partial t$ similar to Fig. 6 for the time moment of 10000 μs.

3. the plate has both anomalous magnetic permeability and anomalous conductivity (combined magnetic and conductive anomaly).

Fig. 2 (top panel) presents the plots of $(\partial H_z)/(\partial t)$ component measured in the center of the loop versus time for Model 1. The solid line corresponds to magnetic field decay for the homogeneous half-space with a resistivity of 100 Ω m (background model). The line formed by crosses is the magnetic response for a purely conductive plate with a resistivity of 1 Ω m (conductive anomaly). An increase in the response occurs within the time interval from 2×10^{-4} to 1×10^{-2} s. The line formed by the stars is the magnetic response for a conductive plate with a resistivity of 10 Ω m (conductive anomaly only). One can see that the anomalous effect is very small in this case. The dotted line is the magnetic response for the case of a purely magnetic plate with $\mu_r = 10$ (magnetic anomaly). This line practically coincides with the solid curve, showing that the anomalous effect is very small in this case as well. Note that the product $\mu_r\sigma$ is the same for the case of the purely conductive anomaly with a resistivity of 10 Ω m (the curve formed by stars), and for the purely magnetic anomaly with a relative magnetic permeability $\mu_r = 10$, and a background resistivity of 100 Ω m (the dotted line in Fig. 2, top panel). The only difference between these two cases is in the presence of the excess magnetic charges at the boundary of the plate. We can conclude that the contribution of these charges is negligibly small, because the corresponding curves practically coincide.

Fig. 2 (bottom panel) shows the results for a combined conductive and magnetic anomaly with different magnetic permeabilities for a plate with a resistivity of 1 Ω m. The solid line corresponds again to magnetic field decay for a homogeneous half-space. The line formed by crosses describes the effect due to eddy currents in a purely conductive anomaly. The dashed line presents the combined effect of anomalous magnetic permeability and anomalous conductivity for $\mu_r = 5$. We can observe an anomaly in the magnetic field decay behavior for a wider time interval than in the case of a purely conductive anomaly. Additional increase in relative magnetic permeability up to 10, leads to further increase of the anomalous effect on $(\partial H_z)/(\partial t)$ decay (shown by the dotted line in Fig. 2, bottom panel) and to shifting this anomaly toward the later time.

We have used numerical modeling to study the electromagnetic field propagation pattern within the model. Figs. 3–8 show the snap-shots of the horizontal component of electric field $E_y(x, z, t)$ and of the time derivative of the vertical component of magnetic field $(\partial H_z(x, z, t))/(\partial t)$ in the vertical plane XZ crossing the horizontal plate in the middle along the axis X. The snap-shots were generated using a finite-difference code for the time moments 100, 1000, and 10 000 μs.

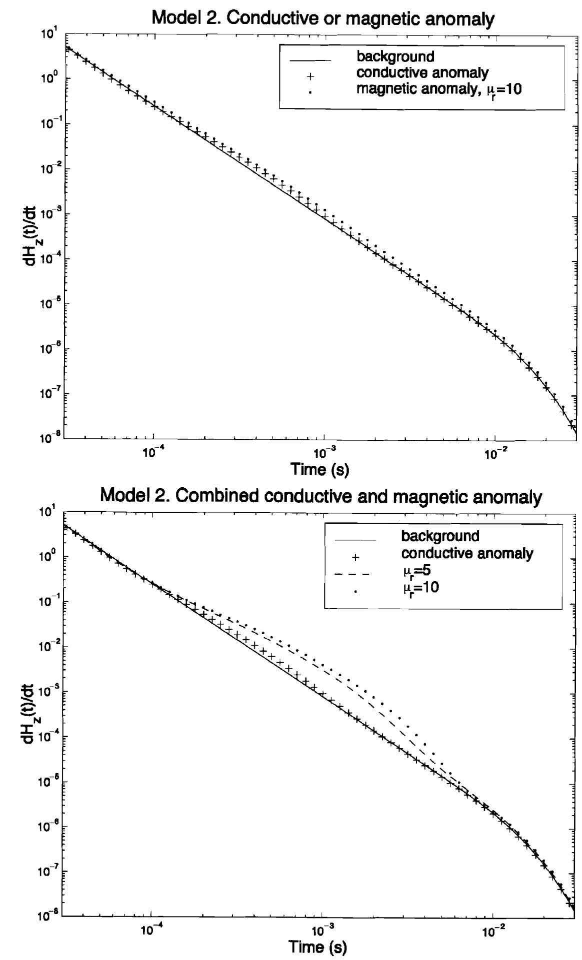

Fig. 9. Top panel: observed field $\partial H_z(t)/\partial t$ versus time for Model 2 above the center of the anomaly. Bottom panel: observed field $\partial H_z(t)/\partial t$ versus time for model 2 above the center of the anomaly for different magnetic permeabilities.

One can see three panels in each of Figs. 3–8. The top panel corresponds to the case of a purely magnetic anomaly ($\rho_2 = \rho_1 = 100$ Ω m) with the relative magnetic permeability of the body $\mu_r = 5$. The bottom panel presents the results for the case of a purely conductive anomaly ($\rho_2 = 1$ Ω m, $\mu_r = 1$), and the middle panel demonstrates the combined effect of magnetic and conductive anomalies ($\rho_2 = 1$ Ω m, $\mu_r = 5$). In the early time (up to 100 μs), the behavior of the electromagnetic field is more or less similar for all three cases. It propagates downward and reaches the plate with the anomalous electromagnetic parameters (Figs. 3 and 6). At 1000 μs, we already see significant differences in field behavior, especially between the models without (top panel) and with (middle and bottom panels) conductive anomalies. In the case of a purely magnetic anomaly, we observe increase of the magnetic field and corresponding increase of the electric field in the anomalous part of the cross-section. However, this increase is smaller than in the presence of the conductive anomaly and is practically confined within the boundaries of the body, as one can see in Figs. 4 and 7.

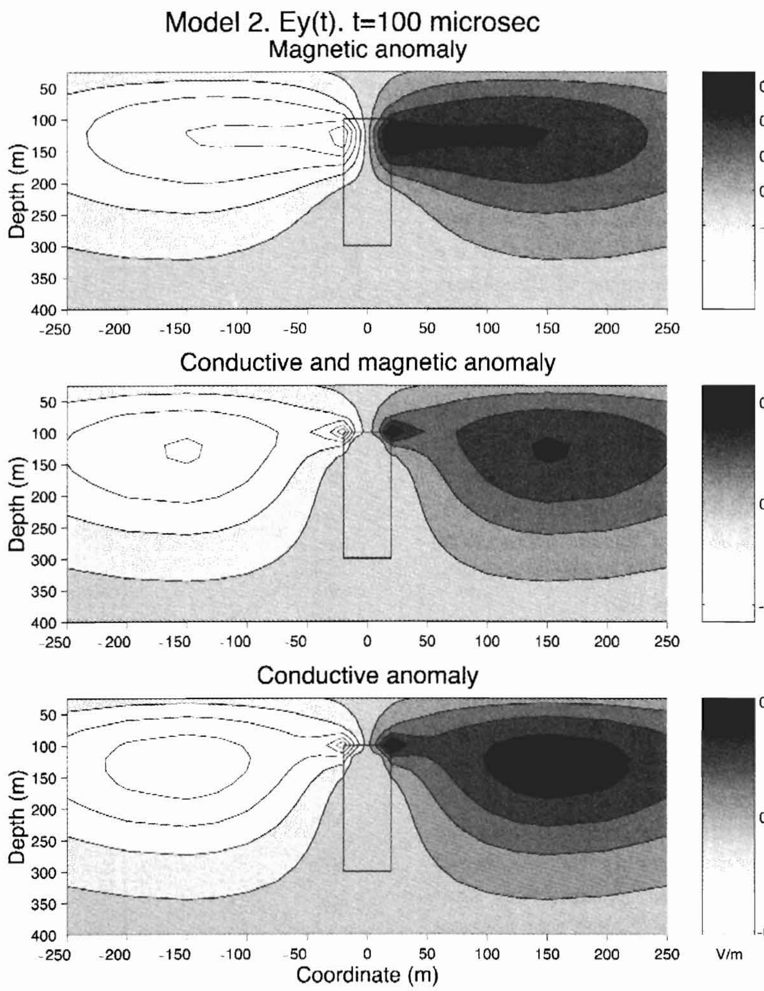

Fig. 10. Model 2. Snap-shots of the horizontal components of electrical field E_y (t, x, z) in the case of a vertical dike for the time moment of 100 μs. The top panel corresponds to the case of a purely magnetic anomaly ($\rho_2 = \rho_1 = 100$ Ω m) with the relative magnetic permeability of the dike $\mu_r = 5$. The bottom panel presents the results for the case of a purely conductive anomaly ($\rho_2 = 1$ Ω m, $\mu_r = 1$), and the middle panel demonstrates the combined effect of magnetic and conductive anomalies ($\rho_2 = 1$ Ω m, $\mu_r = 5$).

Anomalous magnetic fields and electric fields are much stronger in the presence of a conductive anomaly. They form magnetic and electric dipole structures that go beyond the boundaries of the body. That is why the corresponding TDEM field response on the ground is much more significant for conductive and combined magnetic and conductive anomalies than for a purely magnetic anomaly. As one can expect, the contribution of the eddy currents becomes more essential than the effect of purely magnetic polarization. If we go up to 10 000 μs (Figs. 5 and 8), the situation changes. The purely magnetic anomaly is still very small and TDEM response for this case is insignificant. However, the behavior of the electromagnetic field for purely conductive and combined magnetic and conductive anomalies becomes different: for the purely conductive anomaly, eddy currents decay fast and correspondingly, induced electric and magnetic fields practically vanish at the very late time of 10 000 μs. The behavior of the field in the case of the combined magnetic and conductive anomaly is completely different! We still observe a strong magnetic anomaly and strong electric field within the anomalous body (Figs. 5 and 8, middle panels).

This phenomenon can be explained by the fact that the secondary magnetic field associated with the magnetic polarization phenomena is significant over

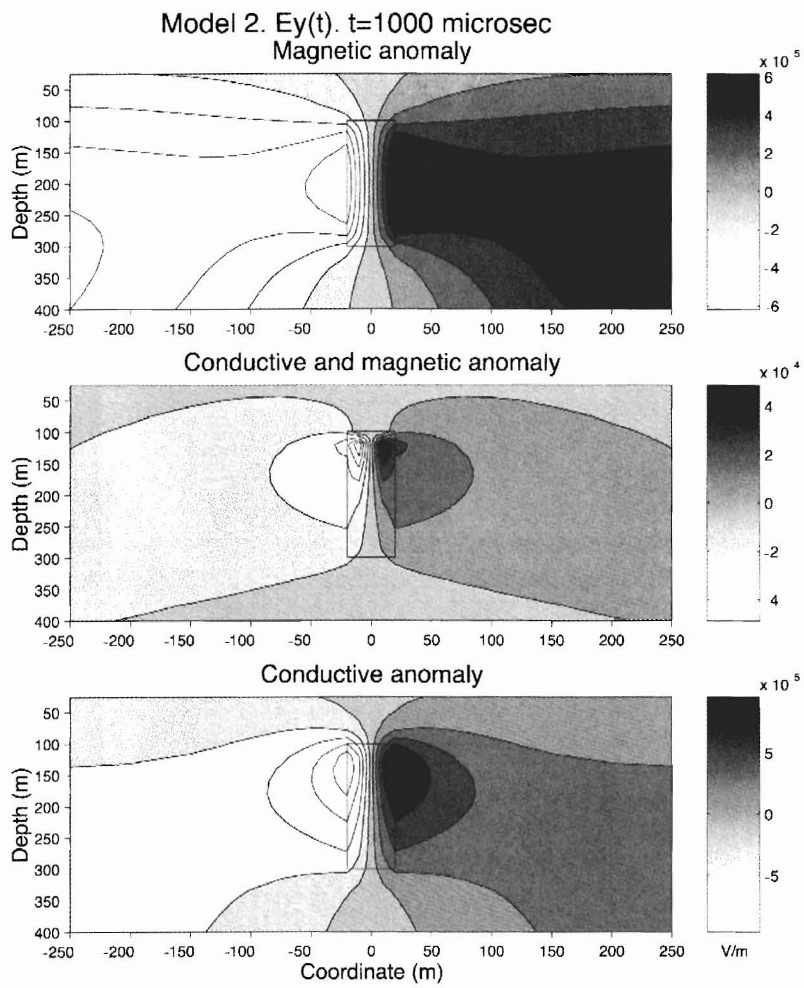

Fig. 11. Model 2. Plots of the horizontal components of electrical field E_y (t, x, z) similar to Fig. 10 for the time moment of 1000 μs.

a much longer time period than eddy currents, because it is connected with the magnetic field itself and not with its time derivative. Eddy currents, strong in the early stages, generate a strong anomalous magnetic field, which is magnified in the magnetized body due to magnetization phenomena. This effect can be understood based on the induction Eq. (6). The term $(\mu_0 \mu_r \sigma\ (\partial E/\partial t))$ in this equation, describing the eddy currents, amplifies significantly in the case of the combined magnetic and conductive anomaly, because both the relative permeability and conductivity increase in this case. With passing time, the eddy currents themselves attenuate quickly, but the generated induced magnetic field stays much longer. This effect results in the shifting of the TDEM anomalous response to the later times, and in its general increase in the case of the combined magnetic and conductive anomalies.

Consider now the results of numerical modeling for Model 2 (Fig. 1, bottom panel). We conducted a set of numerical experiments in which the relative permeability μ_r of the vertical dike was subsequently equal to 1, 5 and 10, and the resistivity of the dike was set to be equal to the background resistivity $\rho_2 = 100\ \Omega$ m, or the dike was a good conductor with $\rho_2 = 1\ \Omega$ m.

Note that the relative permeability value of 10 is extremely high and can be rarely observed in actual

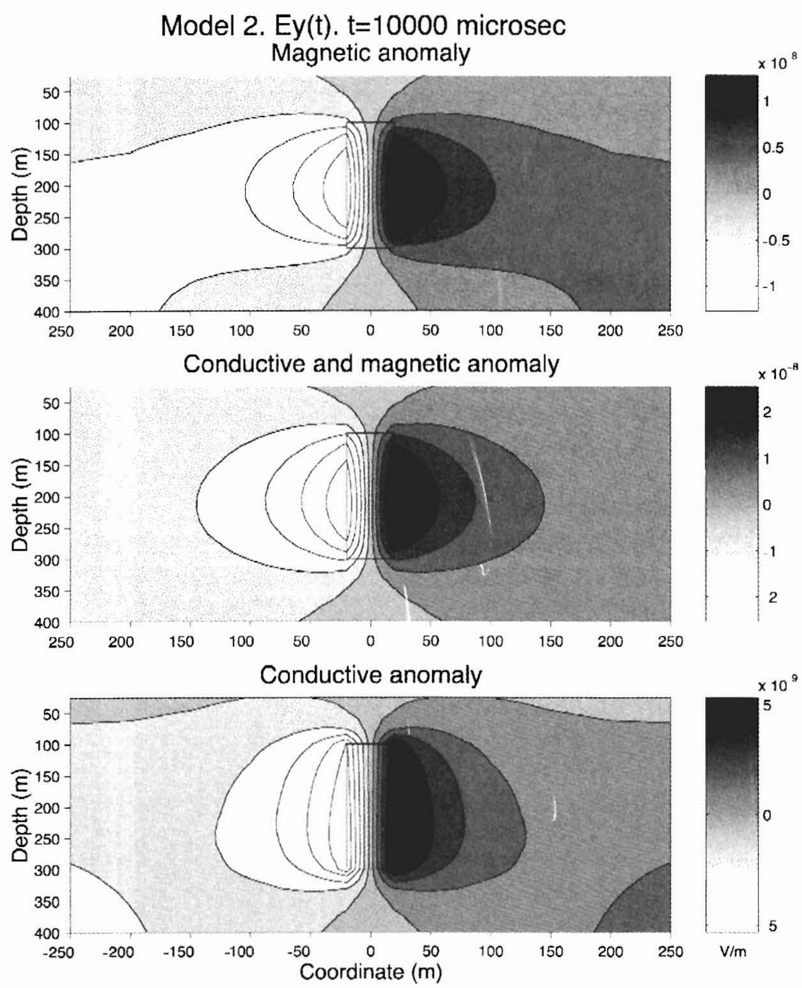

Fig. 12. Model 2. Plots of the horizontal components of electrical field $E_y\ (t,\ x,\ z)$ similar to Fig. 10 for the time moment of 10 000 μs.

rock formations. Nevertheless, we include this value in our analysis to demonstrate that even in this extreme case, the purely magnetic anomaly will still produce a little effect on TDEM data.

Fig. 9 (top panel) presents the plots of the $(\partial H_z)/(\partial t)$ component measured in the center of the loop versus time for Model 2. The solid line corresponds to magnetic field decay for a homogeneous half-space with a resistivity of 100 Ω m (background model). The dotted line is the magnetic response for a case with the purely magnetic permeability anomaly $\mu_r = 10$. This line shows very little anomalous effect in the TDEM response. The line formed by crosses describes the effect due to the eddy current in the purely conductive dike. In this case, it is almost as small as the effect of the purely magnetic anomaly.

Fig. 9 (bottom panel) shows the response for the purely conductive anomaly and for the combined conductive and magnetic anomalies. The resistivity of the dike is equal the $\rho_2 = 1$ Ω m. The solid line corresponds again to magnetic field decay for a

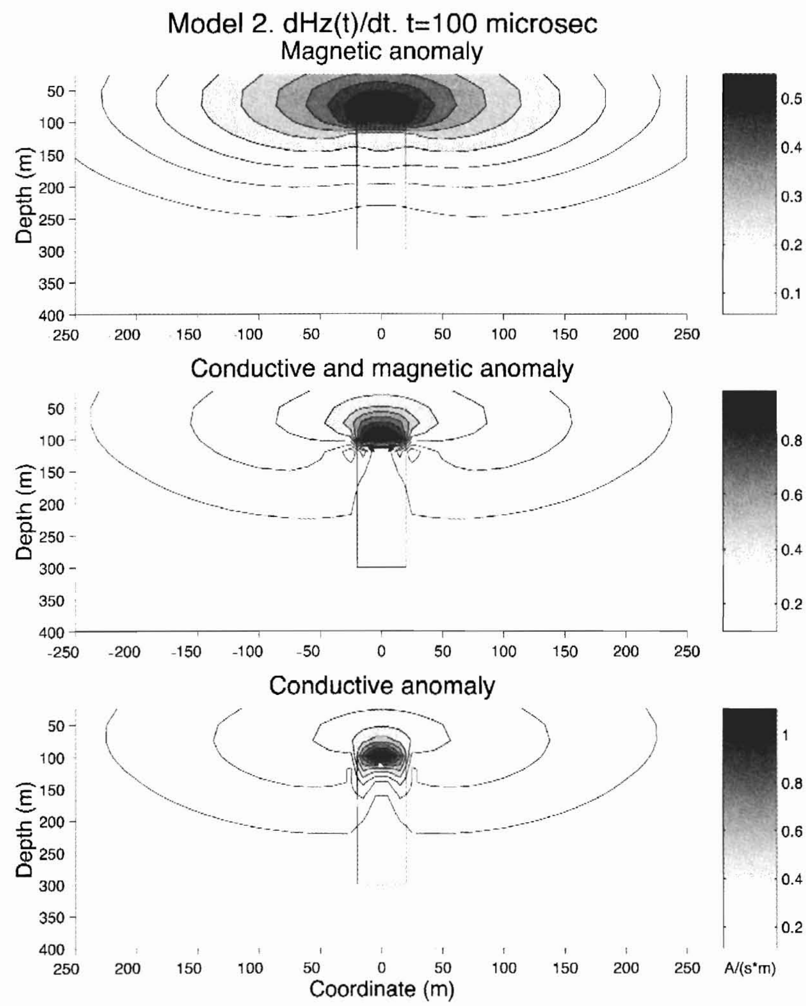

Fig. 13. Model 2. Snap-shots of the vertical components of magnetic field $H_z(t, x, z)/\partial t$ in the case of a vertical dike for the time moment of 100 μs. The top panel corresponds to the case of a purely magnetic anomaly ($\rho_2 = \rho_1 = 100$ Ω m) with the relative magnetic permeability of the dike $\mu_r = 5$. The bottom panel presents the results for the case of a purely conductive anomaly ($\rho_2 = 1$ Ω m, $\mu_r = 1$), and the middle panel demonstrates the combined effect of magnetic and conductive anomalies ($\rho_2 = 1$ Ω m, $\mu_r = 5$).

homogeneous conductive half-space (background model). The line formed by crosses shows again the effect of the purely conductive anomaly. The dashed line presents the combined effect of anomalous magnetic permeability and anomalous conductivity for $\mu_r = 5$. We can observe an anomaly in the magnetic field decay behavior for a rather wide time interval. If we increase the relative permeability of the plate up to 10, the anomalous effect grows significantly and extends till the later times (shown by the dotted line in Fig. 9, bottom panel).

Similar to Model 1, we have studied numerically the electromagnetic field propagation pattern within Model 2. The snap-shots of the horizontal component of electric field E_y (x, z, t), and of the time derivative of the vertical component of magnetic field $(\partial H_z\ (x, z, t))/(\partial t)$ in the vertical plane XZ crossing the vertical dike plate in the middle along the axis X, are shown in Figs. 10–15. We have selected the same time moments as for Model 1: 100, 1000, and 10 000 μs.

The top panels in Figs. 10–15 correspond to the case of a purely magnetic anomaly ($\rho_2 = \rho_1 = 100$ Ω m) with the relative magnetic permeability of the body $\mu_r = 5$. The bottom panels present the results for the case of a purely conductive anomaly ($\rho_2 = 1$ Ω m, $\mu_r = 1$), and the middle panels demonstrate the combined effect of magnetic and conductive anoma-

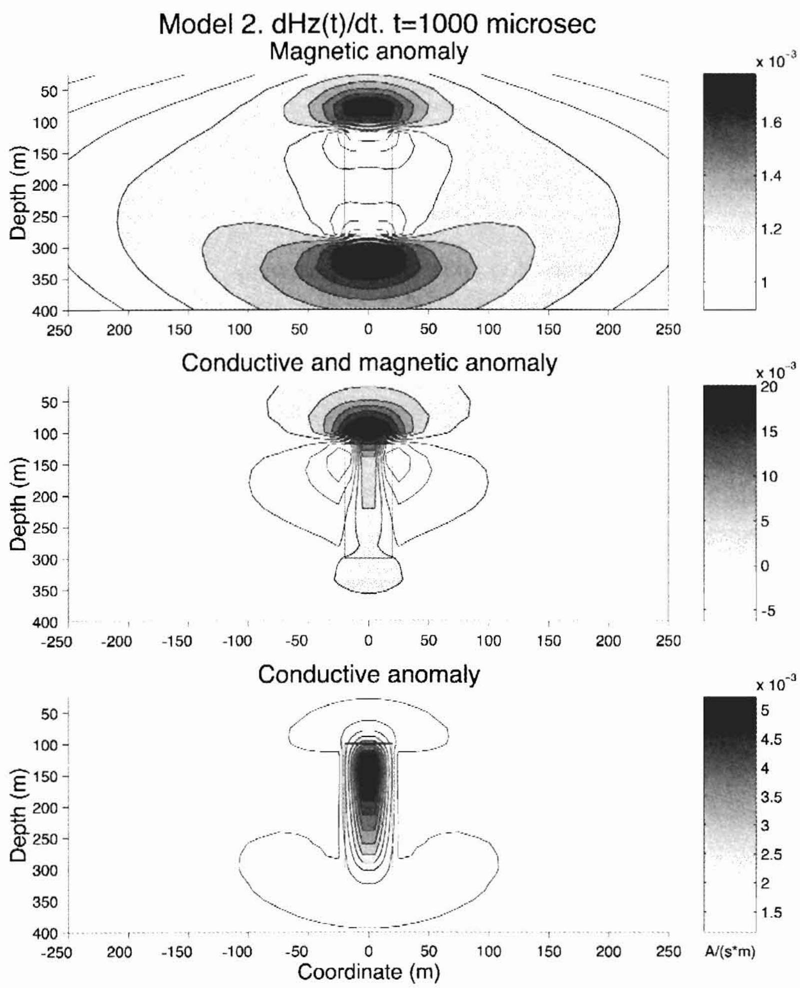

Fig. 14. Model 2. Plots of the vertical components of magnetic field $H_z\ (t, x, z)/\partial t$ similar to Fig. 13 for the time moment of 1000 μs.

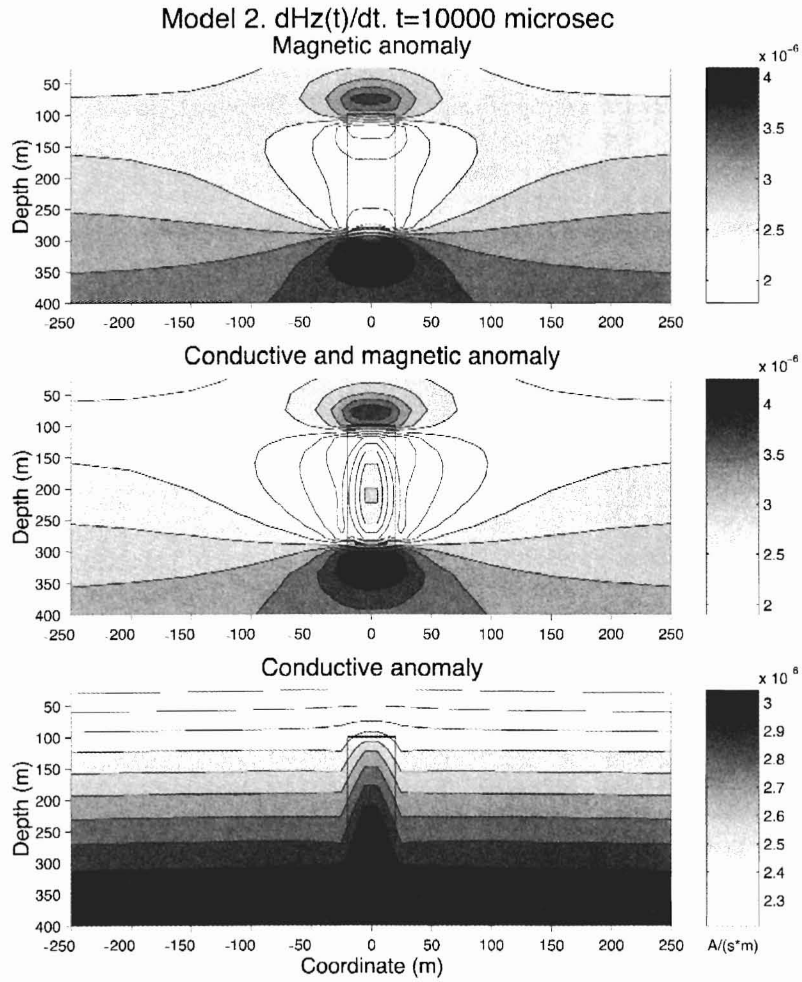

Fig. 15. Model 2. Plots of the vertical components of magnetic field $H_z(t, x, z)/\partial t$ similar to Fig. 13 for the time moment of 10 000 μs.

lies ($\rho_2 = 1\ \Omega$ m, $\mu_r = 5$). We can see again that in the early time (up to 100 μs) the behavior of the electromagnetic field is similar for all three cases. It propagates downward and reaches the top of the dike with the anomalous electromagnetic parameters (Figs. 10 and 13). At 1000 μs, the differences between these three models of different electromagnetic anomalies become significant, especially for the magnetic field components. In the case of a purely magnetic anomaly, we observe two induced magnetic dipoles in the top and in the bottom of the dike with the positive anomaly directed outward of the dike (top panel in Fig. 14). In the case of a purely conductive anomaly, the maximum of the secondary magnetic field is concentrated inside the dike (bottom panel in Fig. 14). This difference is related to the fact that eddy currents tend to reduce the changes in the incident magnetic field B, while the magnetic permeability anomaly caused by paramagnetic material in the dike tends to increase the incident field. We see the combination of these two effects in the middle panel, which corresponds to the combined effect of the conductivity and magnetic permeability anomalies.

The important difference between the modeling results for the horizontal plate and for the vertical dike is that in the last case, the effect of the eddy currents is small and comparable with the effect of the purely magnetic anomaly. It can be explained by the fact that the horizontal transmitter loop generates the horizontal "smoke rings" of the current in the background media, which cannot induce significant eddy currents in the relatively thin vertical dike. Therefore, in the case of the dike, and considering the special geometry of the TDEM survey, the TDEM responses in the ground observations for both the purely magnetic and purely conductive anomalies are relatively small. We observe the same picture for the later time of up to 10 000 μs (Figs. 12 and 15). For purely magnetic anomalies, we still have a small effect which slowly attenuates with time, for purely conductive anomaly eddy currents decay fast and correspondingly induced electric and magnetic fields also disappear at the very late time of 10 000 μs. However, the behavior of the field in the case of combined magnetic and conductive anomalies happens to be very different. We continue to observe significant electric and magnetic anomalies even for a very late time (Figs. 12 and 15, middle panels), because the secondary magnetic field induced by the eddy currents in the earlier time and magnified by the magnetic polarization phenomena continues to be present even for late time observations. This effect is observed on the TDEM decay curves in shifting the anomalous response to the later times.

4. Conclusion

The results of the numerical study have demonstrated that anomalous magnetic permeability of an ore body could result in a significant anomalous effect on the TDEM data. This effect is magnified in the presence of combined conductive and magnetic anomalies. Anomalous magnetic permeability prolongs the anomalous TDEM response to the later times, and increases it overall in comparison with the purely anomalous conductivity effect.

Formal interpretation of TDEM data over simultaneously conductive and magnetized geological structures could produce erroneous results. Therefore, the magnetization effects should be taken into account in developing the methods of TDEM data interpretation in mineral exploration.

We will present a new method for simultaneous inversion of TDEM data for anomalous conductivity and magnetic permeability in the accompanying paper (Zhdanov and Pavlov, 2001).

Acknowledgements

The authors acknowledge the support of the University of Utah Consortium for Electromagnetic Modeling and Inversion (CEMI), which includes 3JTECH, Advanced Power Technologies, Agip, Baker Atlas Logging Services, BHP Minerals, EXXON Production Research, INCO Exploration, Japan National Oil Corporation, MINDECO, MOBIL Exploration and Production Technical Center, Naval Research Laboratory, Newmont Gold, Rio Tinto, Shell International Exploration and Production, Schlumberger–Doll Research, Unocal Geothermal, and Zonge Engineering.

We are thankful to Mr. J. Inman from Kennecott Exploration (Rio Tinto) for fruitful discussions and comments.

We are grateful to the reviewers, Drs. P. Weidelt and Z. Xiong, for their useful comments and recommendations.

References

Fraser, D., 1981. Magnetite mapping with a multicoil airborne electromagnetic system. Geophysics 46, 1579–1593.

Kaufman, A.A., Karinsky, A.D., Wightman, W.E., 1996. Influence of inductive effect on measurements of resistivity through casing. Geophysics 61, 32–34.

Olhoeft, G.R., Strangway, D.W., 1974. Magnetic relaxation and electromagnetic response parameter. Geophysics 39, 302–311.

Strack, K.M., Fanini, O., Maurer, H.-M., Singer, B.S., Tabarovsky, L.A., 1996. Measurements of formation resistivity through a metal casing. GeoArabia-Middle East Petroleum Geosciences 1 (1), 198–210, March GEO'96 Abstracts.

Wang, T., Hohmann, G.W., 1993. A finite-difference time domain solution for three-dimensional electromagnetic modeling. Geophysics 58, 797–809.

Ward, S.H., 1959. Unique determination of conductivity, susceptibility, size, and depth in multifrequency electromagnetic exploration. Geophysics 24, 531–546.

Ward, S.H., Hohmann, G.W., 1988. Electromagnetic Theory for Geophysical Applications: Electromagnetic Methods In Applied Geophysics, 1, Theory. Society of Exploration Geophys., Tulsa, OK, pp. 131–308.

Zhang, Z., Oldenburg, D.W., 1999. Simultaneous reconstruction of 1-D susceptibility and conductivity from electromagnetic data. Geophysics 58, 33–47.

Zhdanov, M.S., Pavlov, D.A., 2001. Analysis and interpretation of anomalous conductivity and magnetic permeability effects in time domain electromagnetic data. Part II: $S\mu$-inversion. Journal of Applied Geophysics 46, 235–248.